Lattice study of dense SU(2) QCD

V.V. Braguta

ITEP

21 August, 2017

Outline:

- The phase diagram at low and moderate density
- Large density: Deconfinement in dense medium

QCD phase diagram

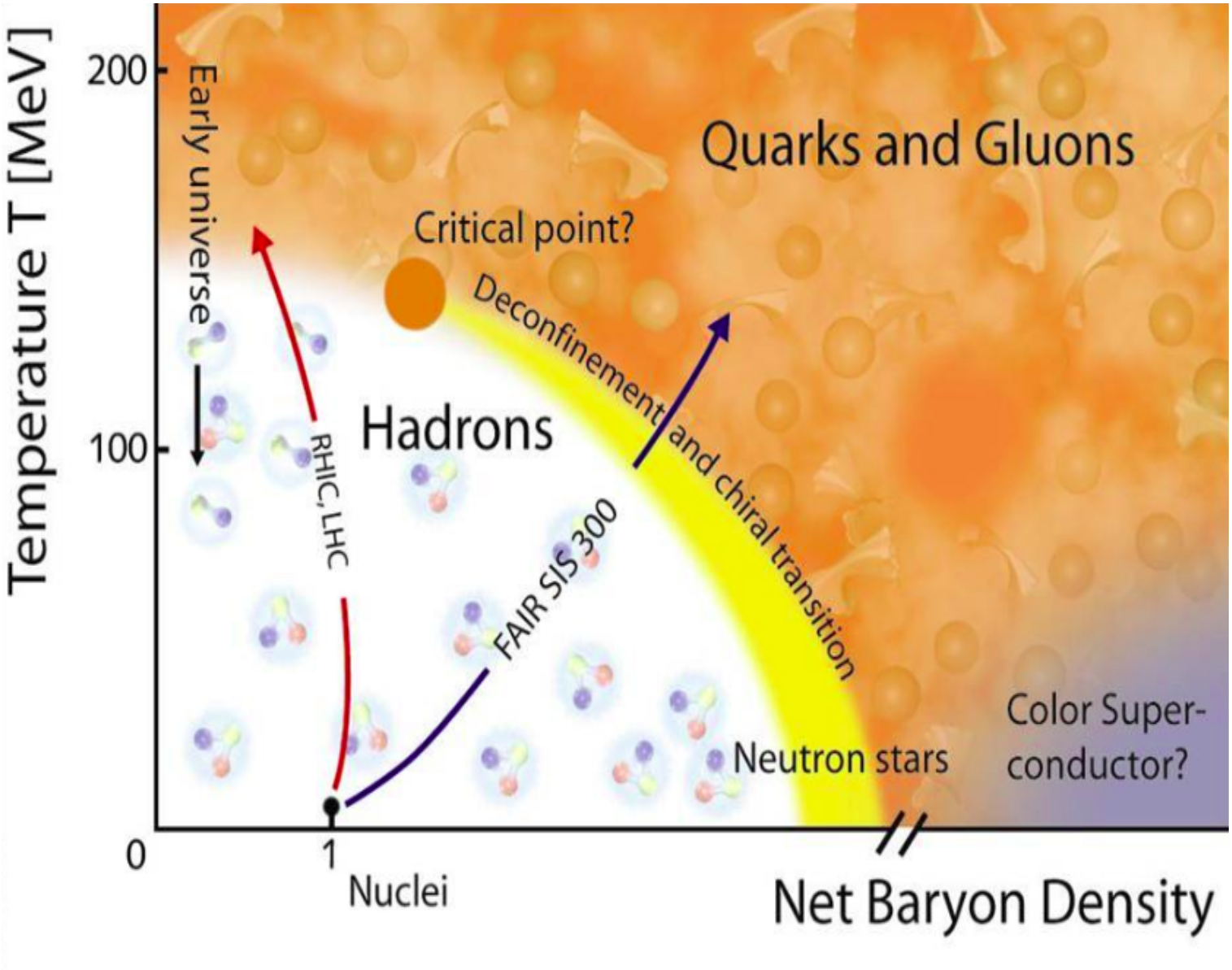

SU(3) QCD

- $Z = \int DUD\bar{\psi}D\psi \ \exp\left(-S_G - \int d^4x\bar{\psi}(\hat{D}+m)\psi\right) =$
  $= \int DU \exp\left(-S_G\right) \times \det\left(\hat{D}+m\right)$
- Eigenvalues go in pairs $\hat{D}: \ \pm i\lambda \Rightarrow$
  $\det\left(\hat{D}+m\right) = \prod_\lambda(\lambda^2+m^2) > 0$
  i.e. one can use lattice simulation
- Introduce chemical potential: $\det\left(\hat{D}+m\right) \to \det\left(\hat{D}-\mu\gamma_4+m\right) \Rightarrow$
  the determinant becomes complex (**sign problem**)

SU(2) QCD

- $(\gamma_5 C\tau_2)\cdot D^* = D\cdot(\gamma_5 C\tau_2)$
- Eigenvalues go in pairs $\hat{D}-\mu\gamma_4$: λ, λ^*
- For even N_f $\det\left(\hat{D}-\mu\gamma_4+m\right) > 0 \ \Rightarrow$ **free from sign problem**

Differences between SU(3) and SU(2) QCD

- The Lagrangian of the SU(2) QCD has the symmetry: $SU(2N_f)$ as compared to $SU_R(N_f) \times SU_L(N_f)$ for $SU(3)$ QCD
- Goldstone bosons ($N_f = 2$) $\pi^+, \pi^-, \pi^0, d, \bar{d}$

Differences between SU(3) and SU(2) QCD

- The Lagrangian of the SU(2) QCD has the symmetry: $SU(2N_f)$ as compared to $SU_R(N_f) \times SU_L(N_f)$ for $SU(3)$ QCD
- Goldstone bosons ($N_f = 2$) $\pi^+, \pi^-, \pi^0, d, \bar{d}$

However, in dense medium:

- **Chiral symmetry is restored**
  symmetry breaking pattern is not important
- **Relevant degrees of freedom are quarks and gluons**
  rather than goldstone bosons

Similarities:

- There are transitions: confinement/deconfinement, chiral symmetry breaking/restoration
- A lot of observables are equal up to few dozens percent:

Topological susceptibility (Nucl.Phys.B715(2005)461):

$\chi^{1/4}/\sqrt{\sigma} = 0.3928(40)$ $(SU(2))$, $\chi^{1/4}/\sqrt{\sigma} = 0.4001(35)$ $(SU(3))$

Critical temperature (Phys.Lett.B712(2012)279):

$T_c/\sqrt{\sigma} = 0.7092(36)$ $(SU(2))$, $T_c/\sqrt{\sigma} = 0.6462(30)$ $(SU(3))$

Shear viscosity :

$\eta/s = 0.134(57)$ $(SU(2))$, $\eta/s = 0.102(56)$ $(SU(3))$

JHEP 1509(2015)082 Phys.Rev. D76(2007)101701

Similarities:

- Spectroscopy (Phys.Rep.529(2013)93)

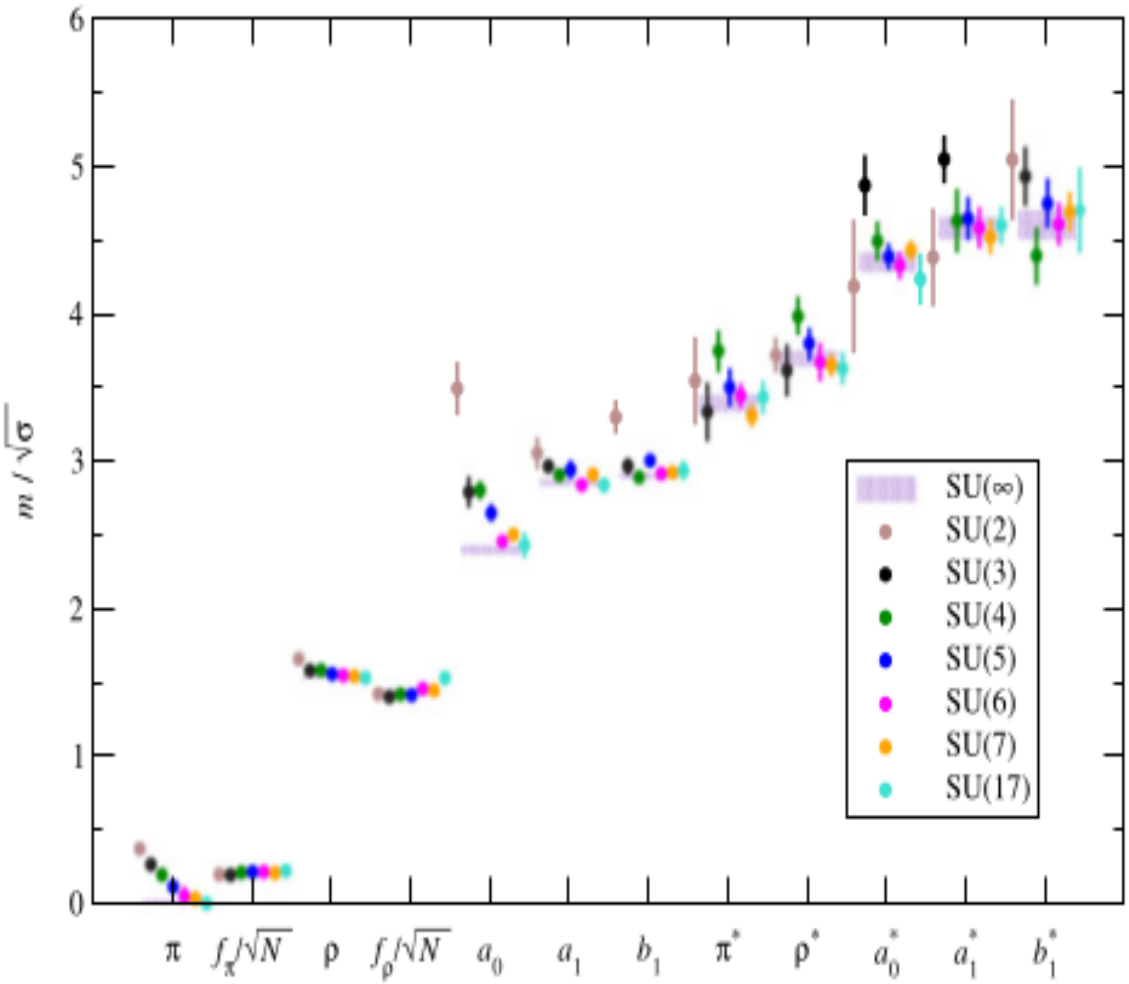

Similarities:

- Thermodynamic properties (JHEP 1205(2012)135)
- Some properties of dense medium (Phys.Rev.D59(1999)094019):

$$\Delta \sim \mu g^{-5} \exp\left(-\frac{3\pi^2}{\sqrt{2}g}\right)$$

To summarize:

- Dense SU(2) QCD can be used to study dense SU(3) QCD
  - Calculation of different observables
  - Study of different physical phenomena
- Lattice study of SU(2) QCD contains full dynamics of real system (contrary to phenomenological models)

To summarize:

- Dense SU(2) QCD can be used to study dense SU(3) QCD
  - Calculation of different observables
  - Study of different physical phenomena
- Lattice study of SU(2) QCD contains full dynamics of real system (contrary to phenomenological models)

The aim: numerical study of dense SU(2) QCD within lattice simulation

$$\mathcal{L} = \bar{\psi}\gamma_\nu D_\nu \psi = \mathrm{i}\begin{pmatrix} \psi_L^* \\ \psi_R^* \end{pmatrix}^T \begin{pmatrix} \sigma_\nu D_\nu & 0 \\ 0 & -\sigma_\nu^\dagger D_\nu \end{pmatrix} \begin{pmatrix} \psi_L \\ \psi_R \end{pmatrix}$$

$$\mathcal{L} = \mathrm{i}\begin{pmatrix} \psi_L^* \\ \tilde{\psi}_R^* \end{pmatrix}^T \begin{pmatrix} \sigma_\nu D_\nu & 0 \\ 0 & \sigma_\nu D_\nu \end{pmatrix} \begin{pmatrix} \psi_L \\ \tilde{\psi}_R \end{pmatrix} = \mathrm{i}\Psi^\dagger \sigma_\nu D_\nu \Psi,$$

$$\Psi \equiv \begin{pmatrix} \psi_L \\ \sigma_2\tau_2\psi_R^* \end{pmatrix} \equiv \begin{pmatrix} \psi_L \\ \tilde{\psi}_R \end{pmatrix}$$

$$\mathcal{L} = \bar{\psi}\gamma_\nu D_\nu \psi = \mathrm{i}\begin{pmatrix} \psi_L^* \\ \psi_R^* \end{pmatrix}^T \begin{pmatrix} \sigma_\nu D_\nu & 0 \\ 0 & -\sigma_\nu^\dagger D_\nu \end{pmatrix} \begin{pmatrix} \psi_L \\ \psi_R \end{pmatrix}$$

$$\mathcal{L} = \mathrm{i}\begin{pmatrix} \psi_L^* \\ \tilde{\psi}_R^* \end{pmatrix}^T \begin{pmatrix} \sigma_\nu D_\nu & 0 \\ 0 & \sigma_\nu D_\nu \end{pmatrix} \begin{pmatrix} \psi_L \\ \tilde{\psi}_R \end{pmatrix} = \mathrm{i}\Psi^\dagger \sigma_\nu D_\nu \Psi,$$

$$\Psi \equiv \begin{pmatrix} \psi_L \\ \sigma_2\tau_2\psi_R^* \end{pmatrix} \equiv \begin{pmatrix} \psi_L \\ \tilde{\psi}_R \end{pmatrix}$$

The symmetry is $SU(2N_f)$

The symmetry of the mass term

$$\bar{\psi}\psi = \begin{pmatrix} \psi_L^* \\ \psi_R^* \end{pmatrix}^T \begin{pmatrix} 0 & 1 \\ 1 & 0 \end{pmatrix} \begin{pmatrix} \psi_L \\ \psi_R \end{pmatrix} = \frac{1}{2} \Psi^T \sigma_2 \tau_2 \begin{pmatrix} 0 & -1 \\ 1 & 0 \end{pmatrix} \Psi + \text{h.c.}$$

- The symmetry is $Sp(2N_f)$

The symmetry of the mass term

$$\bar{\psi}\psi = \begin{pmatrix} \psi_L^* \\ \psi_R^* \end{pmatrix}^T \begin{pmatrix} 0 & 1 \\ 1 & 0 \end{pmatrix} \begin{pmatrix} \psi_L \\ \psi_R \end{pmatrix} = \frac{1}{2} \Psi^T \sigma_2 \tau_2 \begin{pmatrix} 0 & -1 \\ 1 & 0 \end{pmatrix} \Psi + \text{h.c.}$$

- The symmetry is $Sp(2N_f)$
- Pattern of symmetry breaking $SU(2N_f) \rightarrow Sp(2N_f)$

The symmetry of the mass term

$$\bar{\psi}\psi = \begin{pmatrix} \psi_L^* \\ \psi_R^* \end{pmatrix}^T \begin{pmatrix} 0 & 1 \\ 1 & 0 \end{pmatrix} \begin{pmatrix} \psi_L \\ \psi_R \end{pmatrix} = \frac{1}{2} \Psi^T \sigma_2 \tau_2 \begin{pmatrix} 0 & -1 \\ 1 & 0 \end{pmatrix} \Psi + \text{h.c.}$$

- The symmetry is $Sp(2N_f)$
- Pattern of symmetry breaking $SU(2N_f) \to Sp(2N_f)$
- Goldstone bosons $(2N_f)^2 - 1 - N_f(2N_f + 1) = 2N_f^2 - N_f - 1$ $\pi^+, \pi^0, \pi^-, d, \bar{d}$

- Introduce the matrix $\Sigma_{ij} \sim \Psi_i \Psi_j^T$
- $SU(2N_f)$ transformations $\Sigma_{ij} \to U \Sigma U^T$

Chiral lagrangian

$$\mathcal{L}_{\text{eff}} = \frac{F^2}{2} \operatorname{Tr} \partial_\nu \Sigma \, \partial_\nu \Sigma^\dagger - mG \operatorname{Re} \operatorname{Tr}(\widehat{M} \Sigma),$$

Chemical potential

$$L = \bar{\psi}\gamma_\nu D_\nu \psi - \mu\bar{\psi}\gamma_0\psi + m\bar{\psi}\psi$$

$$\bar{\psi}\gamma_0\psi = \begin{pmatrix}\psi_L^* \\ \psi_R^*\end{pmatrix}^T \begin{pmatrix}1 & 0 \\ 0 & 1\end{pmatrix}\begin{pmatrix}\psi_L \\ \psi_R\end{pmatrix} = \Psi^\dagger \begin{pmatrix}1 & 0 \\ 0 & -1\end{pmatrix}\Psi \equiv \Psi^\dagger B \Psi;$$

$$B \equiv \begin{pmatrix}+1 & 0 \\ 0 & -1\end{pmatrix}.$$

Symmetry breaking pattern

- $m = 0$: $SU(2N_f) \to SU_R(N_f) \times SU_L(N_f) \times U_B(1)$

CHPT Lagrangian

$$\begin{aligned}\mathcal{L}_{\text{eff}} &= \frac{F^2}{2}\left[\operatorname{Tr}\nabla_\nu \Sigma \nabla_\nu \Sigma^\dagger - 2m_\pi^2 \operatorname{Re}\operatorname{Tr}(\widehat{M}\,\Sigma)\right] \\ &= \frac{F^2}{2}\operatorname{Tr}\partial_\nu \Sigma\, \partial_\nu \Sigma^\dagger + 2\mu F^2 \operatorname{Tr} B\,\Sigma^\dagger \partial_0 \Sigma \\ &\quad - F^2\mu^2 \operatorname{Tr}\left(\Sigma B^T \Sigma^\dagger B + BB\right) - F^2 m_\pi^2 \operatorname{Re}\operatorname{Tr}(\widehat{M}\,\Sigma).\end{aligned}$$

Vacuum alignment

$$\begin{aligned}\mathcal{L}_{\text{st}}(\Sigma) &= -F^2\mu^2 \operatorname{Tr}\left(\Sigma B^T \Sigma^\dagger B + BB\right) - F^2 m_\pi^2 \operatorname{Re}\operatorname{Tr}(\widehat{M}\Sigma) \\ &= \frac{F^2 m_\pi^2}{2}\left[-\frac{x^2}{2}\operatorname{Tr}\left(\Sigma B^T \Sigma^\dagger B + BB\right) - 2\operatorname{Re}\operatorname{Tr}(\widehat{M}\Sigma)\right],\end{aligned}$$

Vacuum alignment

- Solution at $x = 2\mu/m \to 0$: Σ_c
- Solution at $x \to \infty$: Σ_d

Vacuum alignment

- Solution at $x = 2\mu/m \to 0$: Σ_c
- Solution at $x \to \infty$: Σ_d
- $\Sigma = \Sigma_c cos\alpha + \Sigma_d sin\alpha$

$$V_{eff} = F^2 m_\pi^2 N_f \left[\frac{x^2}{2}(cos2\alpha - 1) - 2cos\alpha \right]$$

Vacuum alignment

- Solution at $x = 2\mu/m \to 0$: $\quad \Sigma_c$
- Solution at $x \to \infty$: $\quad \Sigma_d$
- $\Sigma = \Sigma_c cos\alpha + \Sigma_d sin\alpha$

  $$V_{eff} = F^2 m_\pi^2 N_f \left[\frac{x^2}{2}(cos2\alpha - 1) - 2cos\alpha \right]$$

- Minimum:
  - $x < 1 \quad \alpha = 0,$
  - $x \geq 1 \quad cos\alpha = \frac{1}{x^2}$

Predictions of CHPT

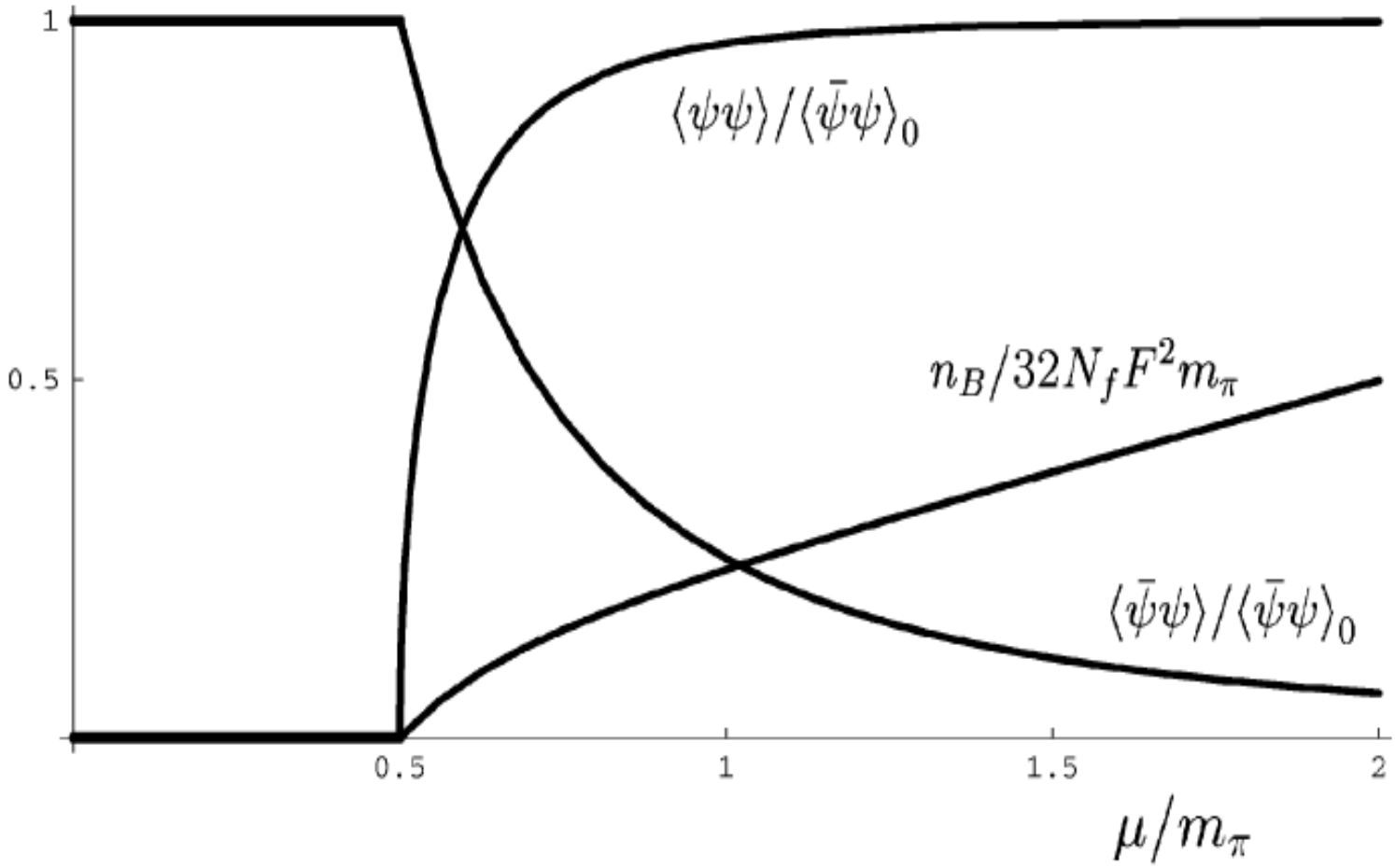

Staggered fermions $N_f = 4$

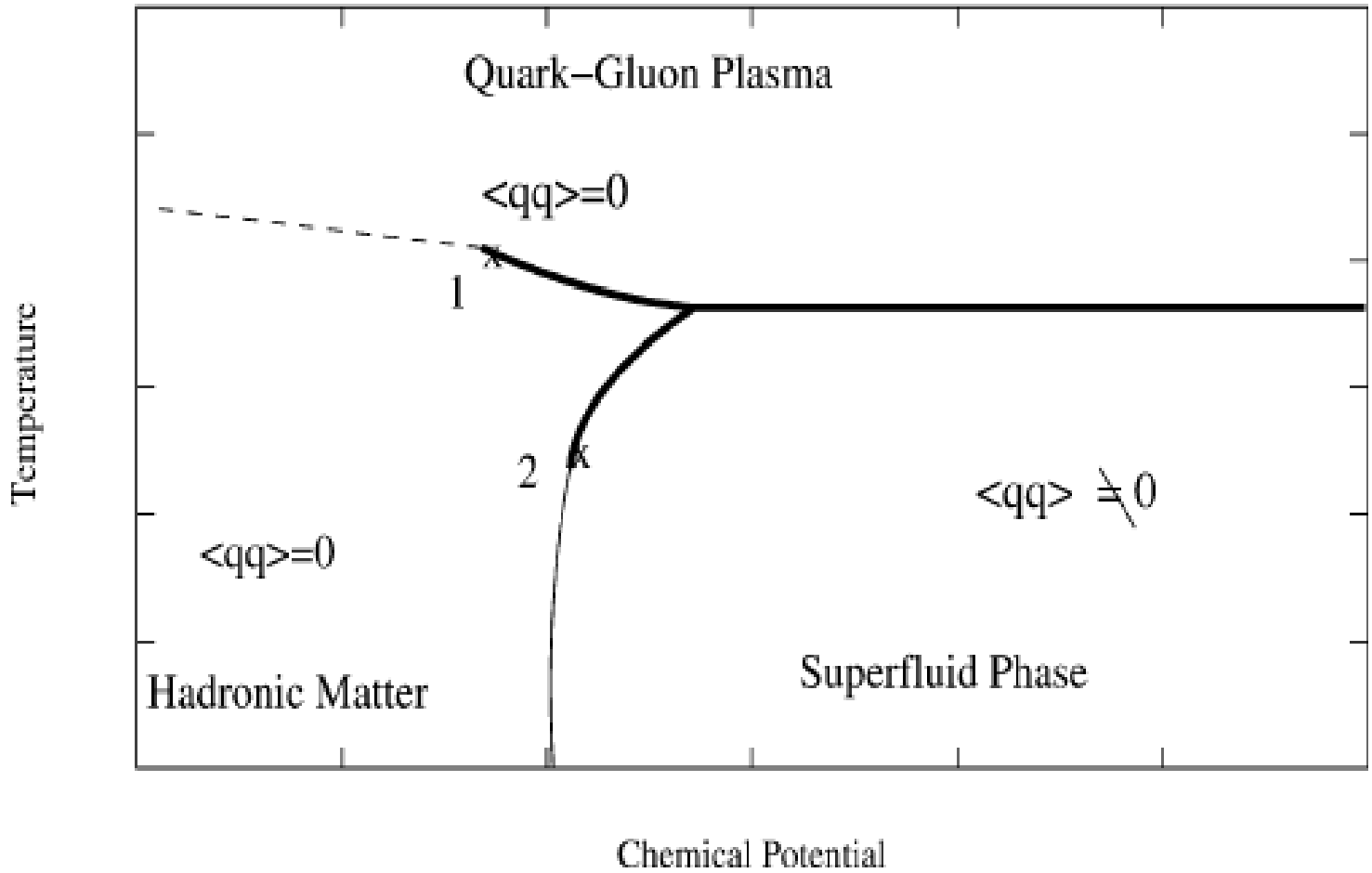

J.B. Kogut, D. Toublan, D.K. Sinclair, Nucl. Phys. B 642 (2002) 181–209

Details of the simulation:

- Staggered fermions with rooting: $N_f = 2$
- Lattice $16^3 \times 32$, $a = 0.11$ fm, $m_\pi = 362(4)$ MeV, $T = 55$ MeV
- Diquark source in the action $\delta S \sim \lambda \psi^T (C\gamma_5) \times \sigma_2 \times \tau_2 \psi$

- The symmetry breaking is different
  - Continuum: $SU(2N_f) \to Sp(2N_f)$
  - Staggered fermions: $SU(2N_f) \to O(2N_f)$
- Correct symmetry is restored in continuum limit
  - Naive limit $a \to 0$: two copies of $N_f = 2$ fundamental fermions
  - Correct β function for $a < 0.17$ fm

Beta function ($\beta = \frac{4}{g^2}$)

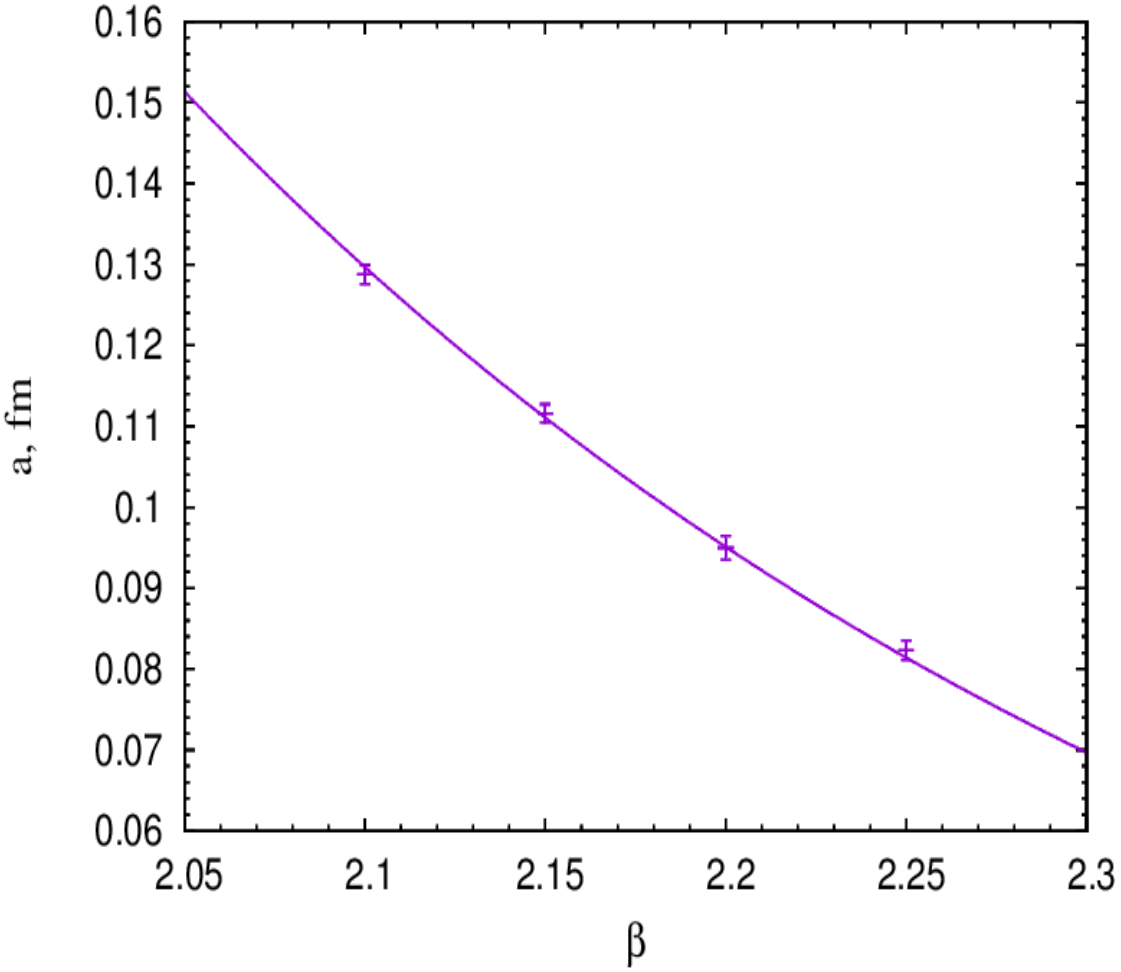

Small chemical potential $\mu < 350$ MeV

Diquark condensate

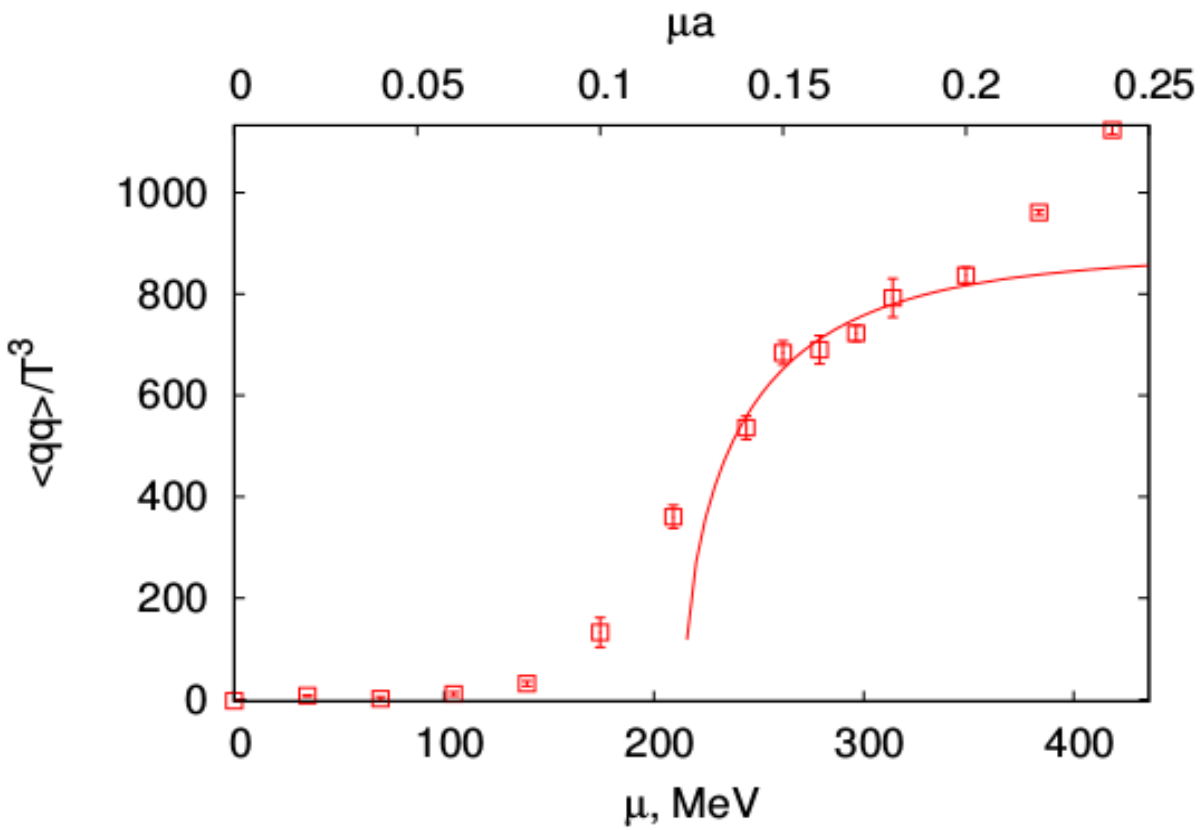

- Good agreement with CHPT $\langle\psi\psi\rangle/\langle\bar{\psi}\psi\rangle_0 = \sqrt{1-\frac{m_\pi^4}{\mu^4}}$
- Phase transition at $\mu \sim m_\pi/2$
- Bose Einstein condensate (BEC) phase $\mu \in (200, 350)$ MeV

Chiral condensate

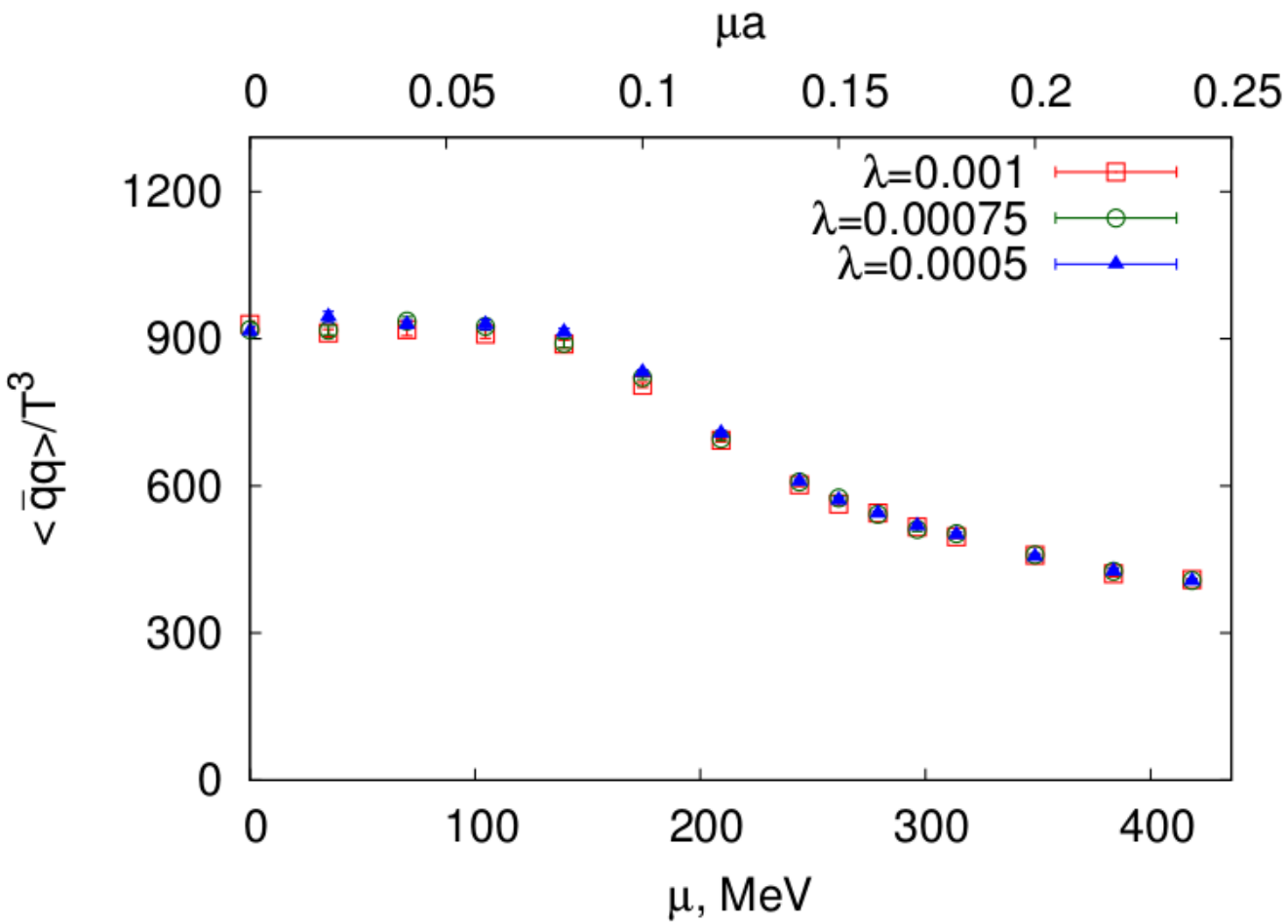

Good agreement with CHPT

Chiral condensate

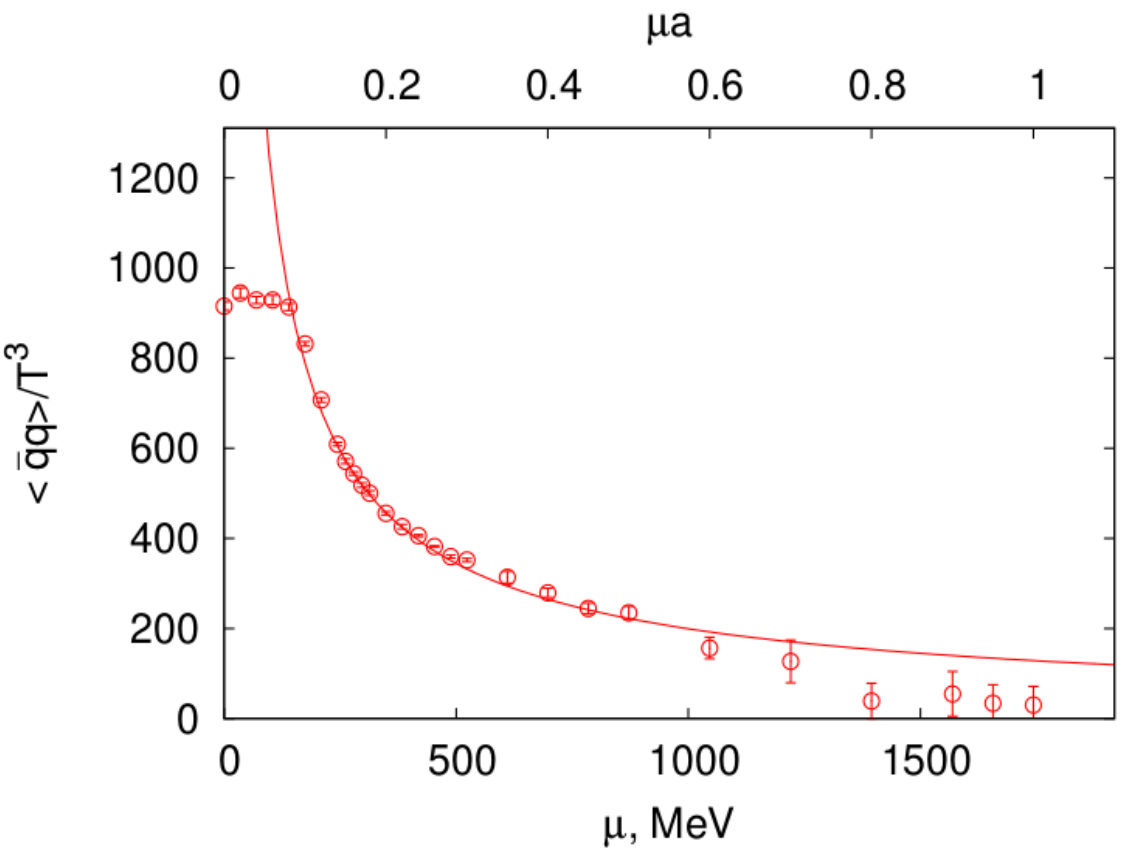

- CHPT prediction $\langle\bar{\psi}\psi\rangle \sim \frac{m_\pi^2}{\mu^2}$
- We observe $\langle\bar{\psi}\psi\rangle \sim \frac{1}{\mu^\alpha}, \alpha \sim 0.6 - 1.0$

Circle relation

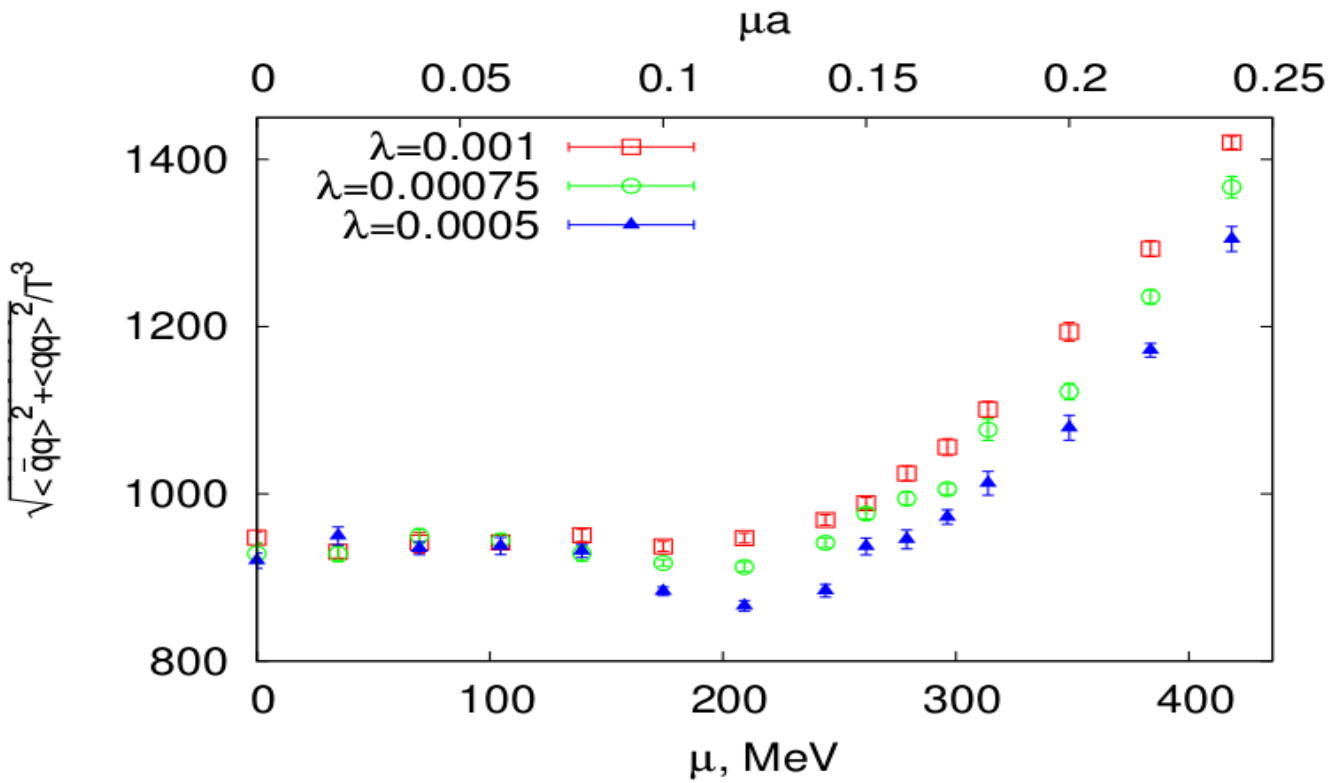

Circle relation: $\langle\bar{\psi}\psi\rangle^2 + \langle\psi\psi\rangle^2 = const$

Baryon density

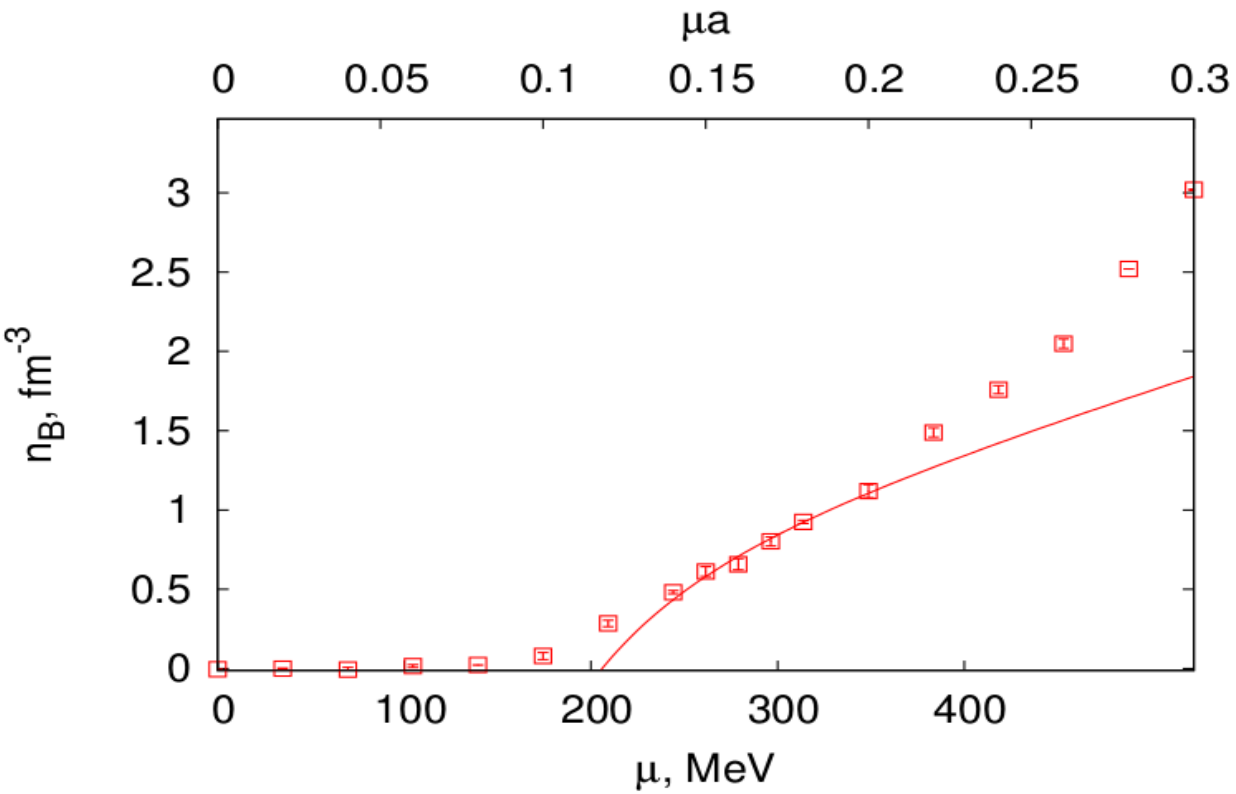

- Good agreement with CHPT $n \sim \mu - \frac{m_\pi^4}{\mu^3}$
- Phase transition at $\mu \sim m_\pi/2$
- Departure from CHPT predictions starts from $n \sim 1$ fm^{-3}
- Transition: dilute baryon gas $\rightarrow$ dense matter
- Baryon size in SU(2) $\sim$ baryon size in SU(3) (agrees with QCD at large N_c)

Large chemical potential $\mu > 350$ MeV

Phase diagram for $N_c \to \infty$

(L. McLerran, R.D. Pisarski, Nucl.Phys. A796 (2007) 83-100)

- Hadron phase $\mu < M_N/N_c$ ($p \sim O(1)$)
- Dilute baryon gas $\mu > M_N/N_c$ (width $\delta\mu \sim \frac{\Lambda_{QCD}}{N_c^2}$)
- Quarkyonic phase $\mu > \Lambda_{QCD}$ ($p \sim N_c$)
  - Degrees of freedom:
    - Baryons (on the surface)
    - Quarks (inside the Fermi sphere $|p| < \mu$)
  - No chiral symmetry breaking
  - The system is in confinement phase
- Deconfinement ($p \sim N_c^2$)

Diquark condensate

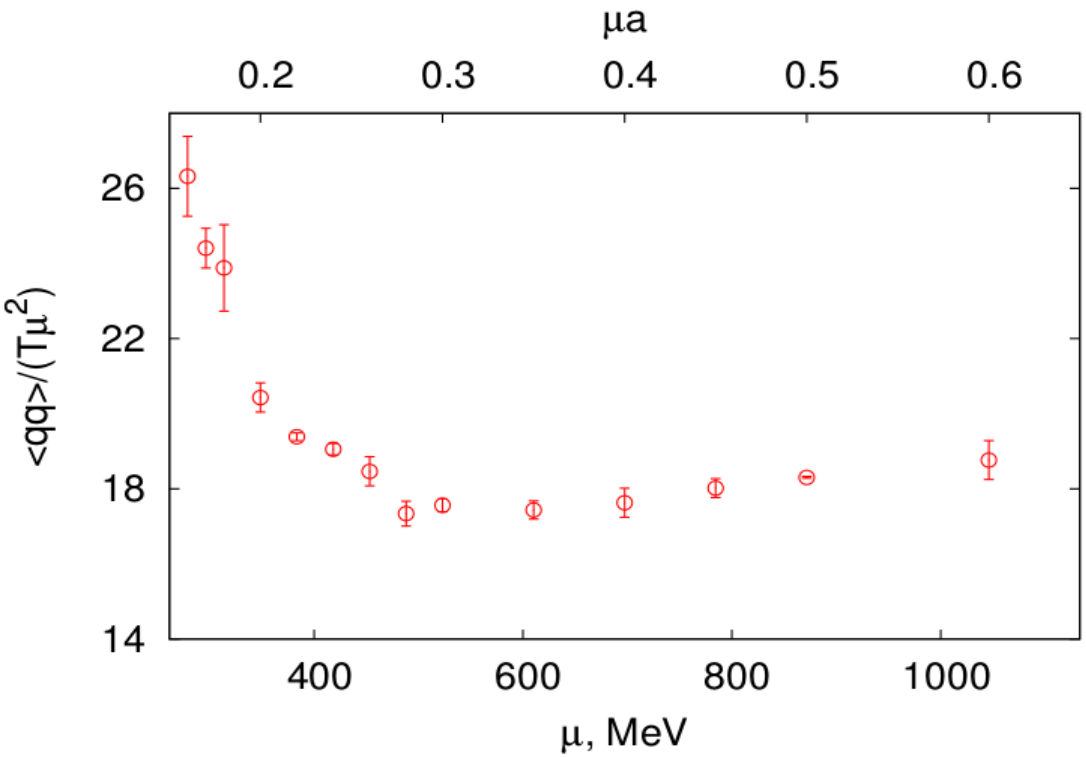

- Bardeen–Cooper–Schrieffer (BCS) phase $\mu > 500$ MeV, $\langle\psi\psi\rangle \sim \mu^2$
- **Baryons (on the surface)**

Baryon density

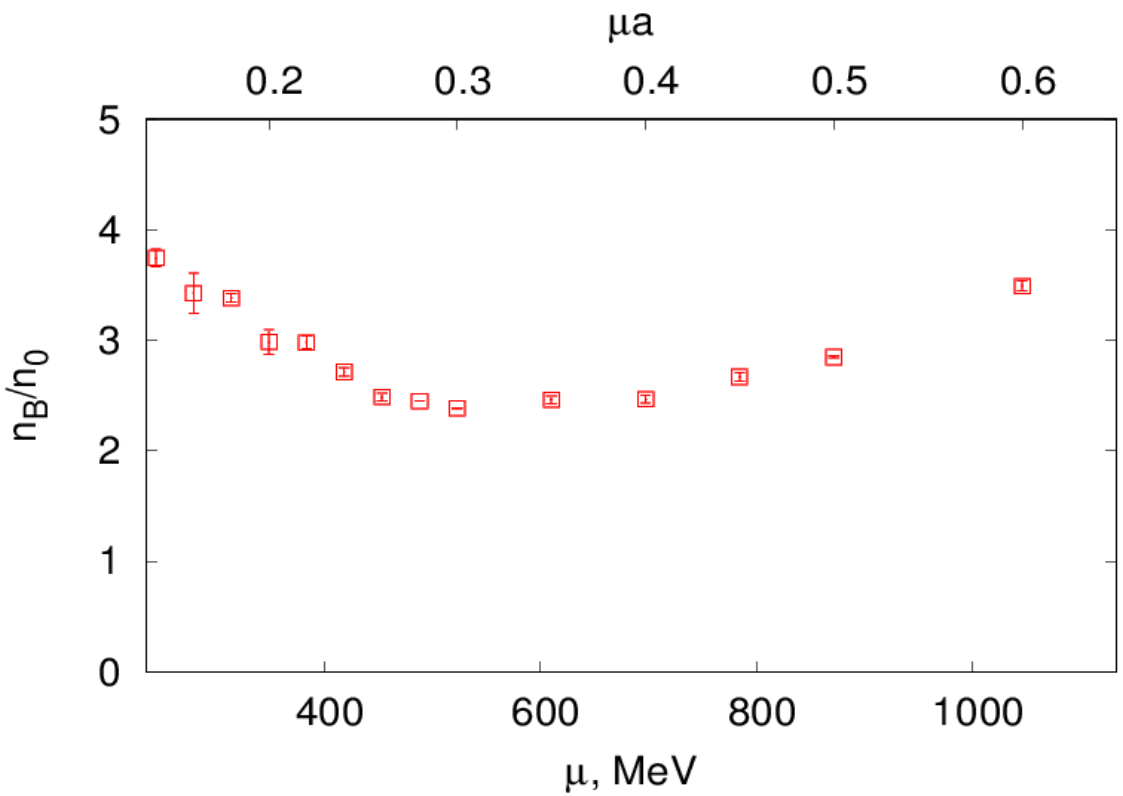

- Free quarks $n_0 = N_f \times N_c \times (2s+1) \times \int \frac{d^3p}{(2\pi)^3}\theta(|p|-\mu) = \frac{4}{3\pi^2}\mu^3$
- **Quarks inside Fermi sphere**
- Quarks inside Fermi sphere dominate over the surface:
  $\frac{4}{3}\pi\mu^3 > 4\pi\mu^2\Lambda_{QCD} \Rightarrow \mu > 3\Lambda_{QCD}$ ($n \sim (5-10)\times$nuclear density)

Chiral condensate (chiral limit $m \to 0$)

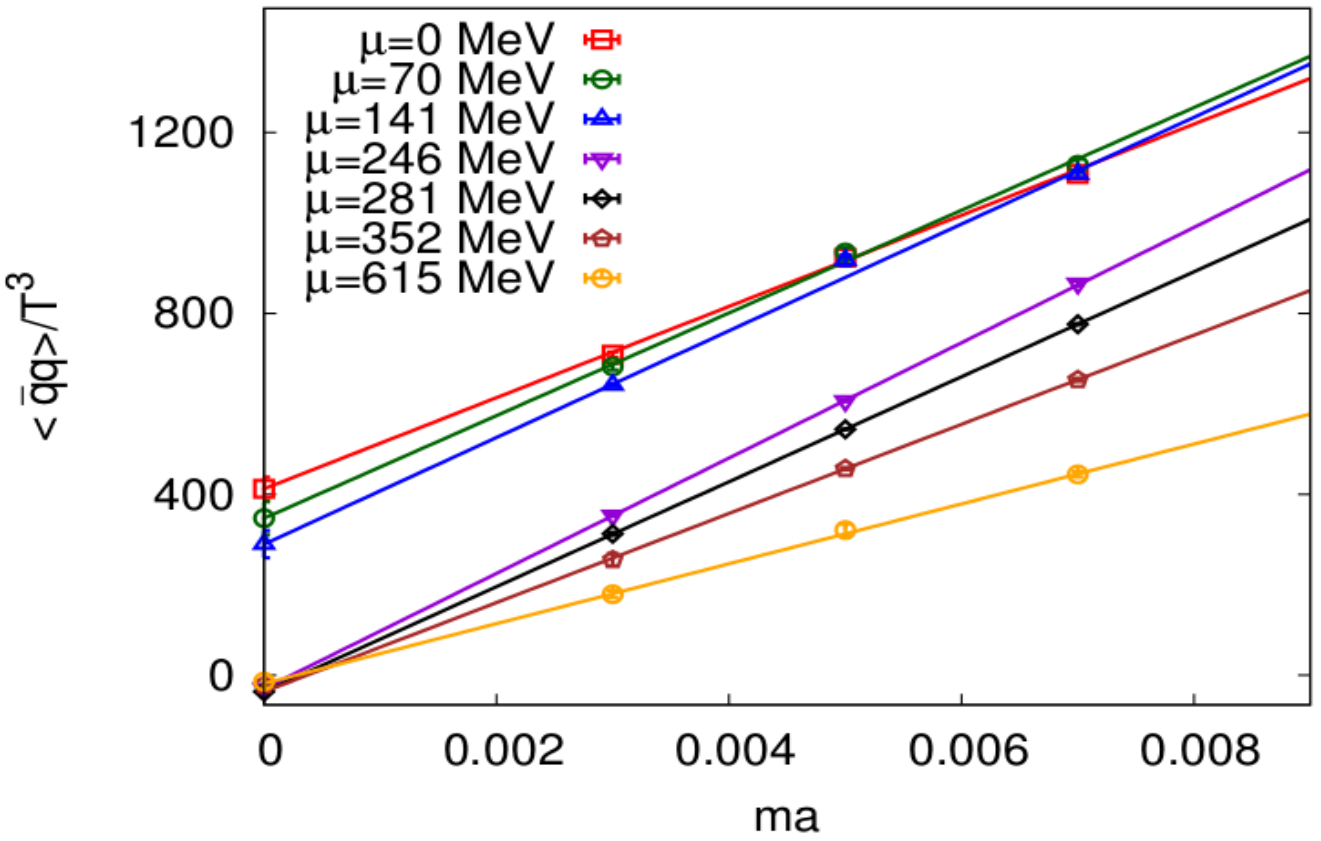

No chiral symmetry breaking

Wilson loop

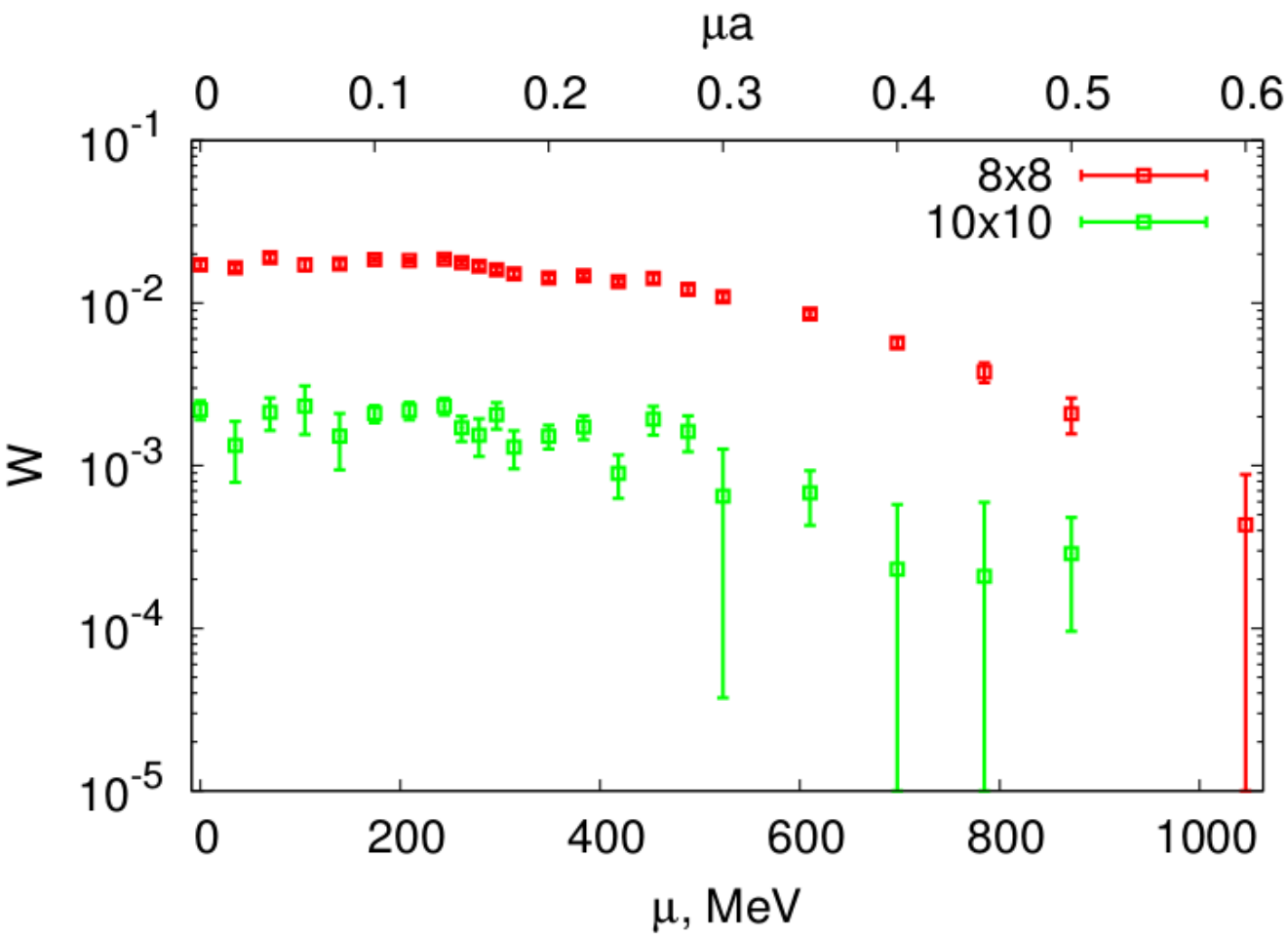

Polyakov loop is zero within the uncertainty of the calculation

Details of the simulation (new study):

- Tree-level improved gauge action
- $a = 0.044$ fm previous study: $a = 0.11$ fm
  $\Rightarrow$ **closer to continuum limit**
  one can reach larger density without lattice artifacts
- $m_\pi = 740(40)$ MeV
  new study: $m_\pi L_s \simeq 5$ previous study: $m_\pi L_s \simeq 3$
  $\Rightarrow$ **Smaller final volume effects**
- Lattices
  - $32^3 \times 32$ ($T \simeq 0$)
  - $32^3 \times 24$ ($T \simeq 186$ MeV)
  - $32^3 \times 16$ ($T \simeq 280$ MeV)
  - $32^3 \times 8$ ($T \simeq 560$ MeV)
- Fixed λ parameter

Details of the simulation (new study):

- Tree-level improved gauge action
- $a = 0.044$ fm previous study: $a = 0.11$ fm
  $\Rightarrow$ **closer to continuum limit**
  one can reach larger density without lattice artifacts
- $m_\pi = 740(40)$ MeV
  new study: $m_\pi L_s \simeq 5$ previous study: $m_\pi L_s \simeq 3$
  $\Rightarrow$ **Smaller final volume effects**
- Lattices
  - $32^3 \times 32$ ($T \simeq 0$)
  - $32^3 \times 24$ ($T \simeq 186$ MeV)
  - $32^3 \times 16$ ($T \simeq 280$ MeV)
  - $32^3 \times 8$ ($T \simeq 560$ MeV)
- Fixed λ parameter

Preliminary results in the next lecture

Conclusion:

- We observe $\mu < m_\pi/2$ hadronic phase
- Transition to superfluid phase $\mu \simeq m_\pi/2$ (BEC)
- $\mu > m_\pi/2, \mu < m_\pi/2 + 150$ MeV dilute baryon gas
- Hadronic phase and BEC phase are well described by CHPT
- Deviation from CHPT from $\mu > 350$ MeV (dense matter)
- BCS phase $\mu \sim 500$ MeV, transition BEC$\rightarrow$BCS is smooth

Conclusion:

- We observe $\mu < m_\pi/2$ hadronic phase
- Transition to superfluid phase $\mu \simeq m_\pi/2$ (BEC)
- $\mu > m_\pi/2, \mu < m_\pi/2 + 150$ MeV dilute baryon gas
- Hadronic phase and BEC phase are well described by CHPT
- Deviation from CHPT from $\mu > 350$ MeV (dense matter)
- BCS phase $\mu \sim 500$ MeV, transition BEC$\rightarrow$BCS is smooth

Monte-Carlo simulation of SU(2) QCD is the best approach to study properties of SU(3) QCD at large baryon density

Conclusion:

- We observe $\mu < m_\pi/2$ hadronic phase
- Transition to superfluid phase $\mu \simeq m_\pi/2$ (BEC)
- $\mu > m_\pi/2, \mu < m_\pi/2 + 150$ MeV dilute baryon gas
- Hadronic phase and BEC phase are well described by CHPT
- Deviation from CHPT from $\mu > 350$ MeV (dense matter)
- BCS phase $\mu \sim 500$ MeV, transition BEC$\rightarrow$BCS is smooth

Monte-Carlo simulation of SU(2) QCD is the best approach to study properties of SU(3) QCD at large baryon density

Next lecture:

Confinement/Deconfinement transition in dense medium